Developmental Biology **215,** 407–419 (1999)
Article ID dbio.1999.9443, available online at http://www.idealibrary.com on IDEAL®

Leaves of *Arabidopsis*

Petra M. Donnelly,* Dario Bonetta,* Hirokazu Tsukaya,† Ronald E. Dengler,* and Nancy G. Dengler*,[1]

**Department of Botany, University of Toronto, Toronto, Ontario M5S 1A1, Canada; and †Institute of Molecular and Cellular Biosciences, The University of Tokyo, 1-1-1 Yayoi, Bunkyo-ku, Tokyo 113-0032, Japan*

Cell cycling plays an important role in plant development, including: (1) organ morphogenesis, (2) cell proliferation within tissues, and (3) cell differentiation. In this study we use a cyclin::β-glucuronidase reporter construct to characterize spatial and temporal patterns of cell cycling at each of these levels during wild-type development in the model genetic organism *Arabidopsis thaliana* (Columbia). We show that a key morphogenetic event in leaf development, blade formation, is highly correlated with localized cell cycling at the primordium margin. However, tissue layers are established by a more diffuse distribution of cycling cells that does not directly involve the marginal zone. During leaf expansion, tissue proliferation shows a strong longitudinal gradient, with basiplastic polarity. Tissue layers differ in pattern of proliferative cell divisions: cell cycling of palisade mesophyll precursors is prolonged in comparison to that of pavement cells of the adjacent epidermal layers, and cells exit the cycle at different characteristic sizes. Cell divisions directly related to formation of stomates and of vascular tissue from their respective precursors occur throughout the period of leaf extension, so that differing tissue patterns reflect superposition of cycling related to cell differentiation on more general tissue proliferation. Our results indicate that cell cycling related to leaf morphogenesis, tissue-specific patterns of cell proliferation, and cell differentiation occurs concurrently during leaf development and suggest that unique regulatory pathways may operate at each level.

***Key Words: Arabidopsis;* cell cycling; cell enlargement; cyclin; leaf development.**

INTRODUCTION

In plants, postembryonic developmental processes are localized to meristems, organized regions of cell proliferation that have the property of self-perpetuation, such as the shoot apical meristem, and to meristematic regions where proliferation occurs, but where all cells eventually differentiate, such as the basal meristem of monocotyledon leaves. Meristems and meristematic regions are the primary locations within the plant where cell cycling occurs, yet the precise role of cell cycling in relation to their function is not clear (Smith, 1996). This is partly a reflection of the nature of plant development itself: processes occur at several levels of organization simultaneously. Cell cycling is intimately associated with organ morphogenesis, proliferation of tissue precursors, and early stages of cell differentiation, but it is likely that cell division plays somewhat different roles at each organizational level and that each level requires unique regulatory pathways.

Leaf morphogenesis has long been a focus of inquiry about the role of cell cycling in the genesis of plant form. In contrast to apical meristems that have an indeterminate, or open-ended, growth plan, leaves of higher plants are determinate in growth, with a finite period of development. The initial form of a typical dicotyledonous leaf is a cylindrical primordium borne on the flank of the shoot apical meristem (Avery, 1933; Foster, 1936; Esau, 1965). The primordium is dorsoventrally symmetrical and flattened on its adaxial side, that toward the meristem. The initial dorsoventral symmetry is accentuated by formation of the leaf blade in its distal region. Blade inception is said to be associated with cycling activity in the "marginal meristem," a region of small cells with densely stained cytoplasm located at the margin between the adaxial and the

[1] To whom correspondence should be addressed at Department of Botany, University of Toronto, Toronto, ON M5S 1A1. Fax: (416) 978-5878. E-mail: dengler@botany.utoronto.ca.

0012-1606/99 $30.00

abaxial leaf surfaces. In addition to a morphogenetic role, the "marginal meristem" is thought to initiate the regular array of tissue layers within the leaf blade; however, earlier studies have reached contradictory conclusions about the duration and relative importance of the marginal meristem in histogenesis (Avery, 1933; Foster, 1936; Esau, 1965; Maksymowych and Wochok, 1969; Poethig and Sussex, 1985; Cusset, 1986).

Between blade inception and leaf maturity, leaves typically expand in area several thousandfold. During the early stages of expansion, proliferative divisions partition leaf tissue into units of optimal size and shape for mature cellular function. In dicotyledons, these proliferative divisions occur in the "plate meristem," a region where precursor cells subdivide anticlinally (perpendicular to the surface) at various angles to give rise to two-dimensional "plates" of cells (Esau, 1965). This pattern maintains the organization of individual tissue layers within the leaf blade, and individual layers form the precursors of epidermal tissue (protoderm), of palisade and spongy mesophyll tissue, and of vascular tissue (procambium). Cell cycling related to differentiation of specific cell types within each layer is superimposed on the more general proliferative cell divisions.

Knowledge of the mechanistic basis of plant cell cycling has provided new ways of studying spatial and temporal patterns of cell division and has opened doors to understanding the regulation of these patterns. Cyclin proteins are particularly good markers for cell proliferation since they show patterns of accumulation and destruction that are specific to different phases of the cell cycle (Hemerley *et al.*, 1992; Ferreira *et al.*, 1994a,b; Renaudin *et al.*, 1996; DeVeylder *et al.*, 1998). In *Arabidopsis*, 5 of the 11 cyclins reported thus far show significant homology to mitosis-specific cyclins, including the presence of a cyclin box and a N-terminus destruction motif (Hemerly *et al.*, 1992; Ferreira *et al.*, 1994a; De Veylder *et al.*, 1998). Both *in situ* hybridization experiments with intact *Arabidopsis* tissue and analysis of β-glucuronidase (GUS) reporter expression in synchronous cell cultures of tobacco indicate that the cyclin transcript *cyc1At* is most abundant during G2 and M phases of the cycle (Hemerly *et al.*, 1992; Shaul 1996c). *In situ* hybridization experiments also show that plant cyclin genes are expressed in localized spots of one or two cells, with high frequencies of labeled cells in apical meristems, young leaf primordia, and vascular traces (Fobert *et al.*, 1994; Kouchi *et al.*, 1995; Doerner *et al.*, 1996; Shaul *et al.*, 1996b).

In this study we make use of a *cyc1At::GUS* reporter construct to follow spatial and temporal patterns of cell division in developing leaves of wildtype (Columbia) *Arabidopsis thaliana*. Our primary goal is to evaluate these patterns in relation to leaf morphogenesis, tissue proliferation, and cell differentiation. We emphasize the patterns of proliferative cell division and cell enlargement in the two layers of the leaf blade that will give rise to the adaxial epidermal and palisade mesophyll tissues, as representative of other tissue-specific patterns. This detailed characterization provides a baseline for mutant characterization and provides essential information for future understanding of the regulation of the plant cell division cycle, particularly as it plays a role in plant organs with a determinate pattern of development.

MATERIALS AND METHODS

Plant Material

Seeds of transformed *A. thaliana* (ecotype Columbia) carrying the *cyc1At::GUS* reporter construct (equivalent to *Arath;CycB1;2;* Renaudin *et al.*, 1996) were kindly provided by John L. Celenza, Boston University. This GUS construct consists of the *cyc1At* promoter plus the region coding for the first ~150 amino acids of *cyc1At*, which includes the cyclin destruction box (CDB). The CDB is fused in frame to GUS, so that CDBGUS protein is degraded at the end of mitosis, similar to a mitotic cyclin (J. L. Celenza, personal communication). Seeds were sterilized with 20% bleach in 0.01% SDS, rinsed, and stored for 1 week at 4°C before being plated on agar with 0.5× MS salts and 15 μg/ml kanamycin. Plates were placed in a Conviron E15 growth chamber with 14:10 h day:night cycle and 22°C. Seedlings were transplanted to sterilized Promix 10 days postgermination and maintained in the same chamber.

Growth of the first 10 rosette leaves was followed for 10 plants by measuring leaf blade and petiole every second day for 35 days. The eighth rosette leaf (Leaf 8) was selected for more detailed study, as it is formed well after the transition from the juvenile to adult phase (Telfer and Poethig, 1994) and has more strongly developed palisade mesophyll than earlier-formed leaves (unpublished observations). Since variation in the lengths of the first 10 rosette leaves was relatively small at each time point, we used a chronological time scale to characterize Leaf 8 development.

Detection of GUS Activity

Histochemical detection of GUS activity was carried out using 5-bromo-4-chloro-3-indolyl-β-D-glucuronide (X-Gluc) as a substrate. Leaf tissue first was placed in 90% acetone on ice for 15 min and then in X-Gluc buffer solution (750 μg/ml X-Gluc, 100 mM $NaPO_4$ (pH 7), 3 mM $K_3F_3(CN)_6$, 10 mM EDTA, 0.1% Nonidet-P40) under vacuum (500 mm Hg) for 16 h at room temperature. Treatment at room temperature and increased concentration of $K_3F_3(CN)_6$ reduced diffusion of the water-soluble indoxyl intermediate and enhanced oxidative dimerization to the dichlorodibromo indigo blue precipitate (DeBlock and Van Lijsebettens, 1997).To clarify subcellular localization of GUS activity and better visualize nuclei, cleared leaf tissues were stained with 0.1% Hoechst 33258 in Tris-buffered saline.

Tissue Preparation for Microscopy

After GUS detection, leaf tissue was rinsed in 70% ethanol and cleared in 8:2:1 (chloral hydrate:glycerol:water) and mounted in the same solution on microscope slides. Additional tissue was fixed in FAA (formalin:acetic acid:70% ethanol, 1:1:18) after GUS detection, dehydrated through an ethanol series, and embedded in Historesin. For Days 16, 20, and 24, leaf tissue was also embedded in Spurr resin. Tissue was sectioned at 2 μm with a RMC

Microtome and Microstar diamond knife and counterstained with 0.01% aqueous safranin for Historesin or 0.05% toluidine blue O for Spurr resin. Serial cross sections through the shoot apex region were used to observe leaves at Days 0 to 4; leaf lengths were calculated by counting the number of serial sections in which a primordium appeared and multiplied by section thickness. Slides were examined under bright-field optics on a Reichert Polyvar microscope and recorded using Kodak Gold or T-Max film. Between six and nine replicate leaves (each Leaf 8 from a different seedling) are included in the data for each time point during leaf expansion.

Since precocious trichome formation obscures the earliest stages of leaf development, we used *A. thaliana* Columbia carrying the mutant *glabra* (*gl1*) allele to illustrate these stages by scanning electron microscopy. Tissue was fixed in FAA, dehydrated, critical point dried, and observed with a Hitachi S520 scanning electron microscope.

In Situ Hybridization

In situ hybridization with digoxigenin-labeled RNA probes in wild-type plants was used to verify the pattern of GUS activity seen in plants transgenic for the *cyc1At::GUS* reporter construct. Antisense and sense *cyc1At* probes were generated from a pBluescript II KSt vector cut with *Bss*HII and T3 or T7 RNA polymerase, following the Boehringer Mannheim protocol. Probes were ca. 1.6 kb in length and were hydrolyzed to ca. 100 bp prior to hybridization. Tissue was fixed in 4% paraformaldehyde, dehydrated in an ethanol–xylene series, embedded in Paraplast^{+}, sectioned at 7μm, and mounted on poly-L-lysine-coated slides. Hybridization procedure followed the Drews and Okamura protocol (1996).

Quantitative Observations

The frequency of cells localizing GUS activity was assessed at five locations along the length of the leaf blade (0, 25, 50, 75, and 100% of the distance from base to apex) and approximately midway between the leaf midvein and margin by photographing cleared leaves under differential interference contrast optics and focusing on either the adaxial epidermis or the palisade mesophyll layers. The total cell number and number with GUS activity in each layer were counted in an area of 0.02 mm^2 and expressed as the "cyclin index" (No. cells with GUS activity/No. total cells $\times$ 100).

Cell size was assessed from photographs of cleared leaves. The paradermal area of 10 contiguous adaxial epidermal cells (omitting differentiating guard cells, trichome cells, and trichome-associated support cells, but including meristemoids) and 10 contiguous cells in the palisade mesophyll layer were measured using a GTCO digitizing tablet and Sigmascan (Jandel Scientific, Inc.) software and plotted using Sigmaplot (Jandel Scientific, Inc.). Since we wanted to emphasize within-sample variability in cyclin index and cell area data and how variability changes over time, the data are presented in the form of box graphs which display the mean; median; 10th, 25th, 75th, and 90th percentiles; and outlier points for each sampling time (Figs. 9 and 11; Cleveland, 1985).

RESULTS

Localization of GUS Activity

The GUS reporter for cyclin gene *cyc1At* expression was detected in single cells that were usually isolated from other GUS-expressing cells, even when labeling was dense (Figs. 1A–1D). Most labeled cells are in interphase, but ca. 5% of GUS-accumulating cells are in mitosis, with telophase being the most frequently observed phase (Fig. 1B). We interpret these results as being consistent with the demonstration that B-type cyclins are expressed during G2 and mitosis specifically and that cyclin is degraded after mitosis. Such cell-specific localization is similar to that observed in other GUS reporter construct and *in situ* hybridization analyses of cyclin expression in vegetative and floral meristems (Fobert *et al.*, 1994; Kouchi *et al.*, 1995; Doerner *et al.*, 1996; Shaul *et al.*, 1996a).

When sections of developing leaves were probed with DIG-labeled *cyc1At* antisense RNA probes, the pattern of DIG detected in the tissue was similar to that seen for GUS labeling in leaves of comparable ages (Figs. 1D and 1E). Individual cells in the protodermal, ground meristem, and procambial tissues showed DIG label in a diffuse pattern across the leaf blade. Sense RNA control probes did not label individual cells intensely (Fig. 1F).

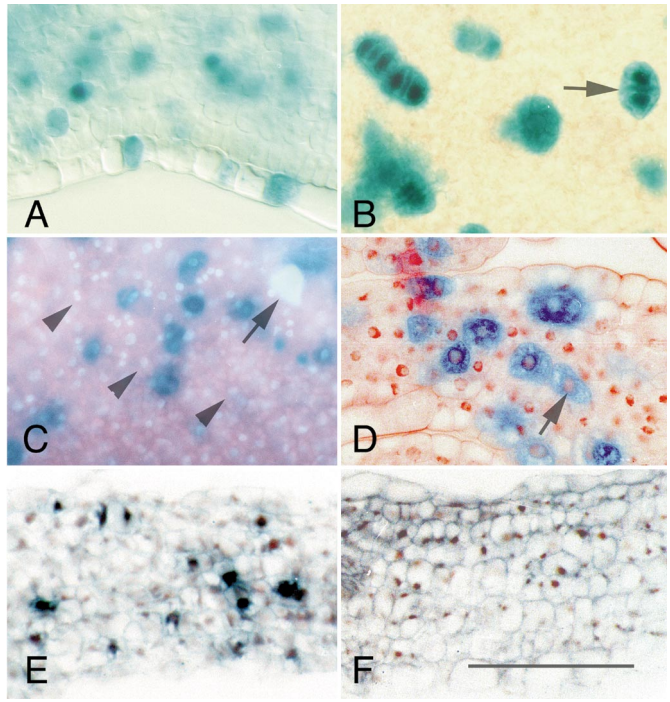

FIG. 1. Localization of GUS activity in developing leaves of *Arabidopsis*. (A and B) Cleared leaves viewed with bright-field microscopy. Arrow indicates mitotic figure. (C) Cleared leaf stained with Hoechst 33258 and viewed with fluorescence microscopy. Arrowheads indicate nuclei of protoderm cells. Note large polytene nucleus of developing trichome cell in upper right arrow. (D) Section of Historesin-embedded Day 4 leaf. Arrow indicates nucleus. (E) *In situ* hybridization with DIG-labeled antisense probe. (F) *In situ* hybridization of paraffin-embedded tissue with DIG-labeled sense probe. Scale, 50 μm.

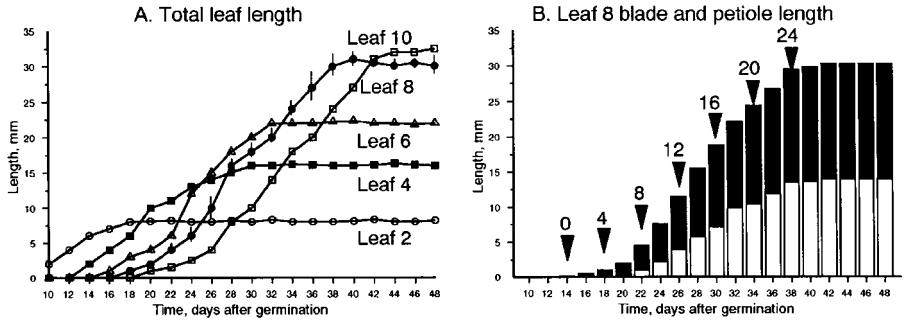

FIG. 2. Time course of expansion of *Arabidopsis* leaves. (A) Increase in mean total length of Leaves 2, 4, 6, 8, and 10 with time. (B) Mean blade (black) and petiole (white) lengths in expanding Leaf 8. Arrowheads indicate times of Leaf 8 tissue sampling for this study.

Leaf Expansion

Under our growth conditions, Leaf 8 is initiated about 14 days after germination (Fig. 2A). It becomes macroscopically visible 16–18 days after germination, elongates slowly at first and then more rapidly between 22 and 36 days after germination; elongation ceases by the 38th day (Fig. 2A). The relative proportions of leaf blade and petiole changed during expansion: the blade expands more rapidly during the early part of leaf growth (up to Day 8), while the petiole undergoes more rapid expansion after this stage (Fig. 2B). For the purposes of this study, we designated the 14th day after germination Day 0 of Leaf 8 development and numbered developmental stages from Day 0 (Fig. 2B).

Temporal and Spatial Patterns of Cyclin Accumulation

At Day 0, Leaf 8 primordia range from flattened cylinders less than 50 μm in length (Fig. 3A) to more strongly dorsoventral structures with a blade and a basal constricted region that will form the petiole more than 250 μm in length (Fig. 3B). In whole mounts of developing leaves, the distribution of cells with GUS activity is uniform (Fig. 3C). In cross-sectional view, GUS-expressing cells occur in a diffuse pattern in protoderm, mesophyll precursors, and procambium, with greater frequency toward the adaxial side of the leaf (Figs. 3D and 3E). In primordia about 50 μm in length, cells in a marginal position show strong GUS activity (Fig. 3D).

At Day 4, the frequency of cells with GUS activity is high throughout the leaf blade, with limited areas of reduced activity near the apex, petiole, and basal portion of the midvein (Fig. 4A). In blade cross sections, individual GUS-accumulating cells are diffusely distributed between midvein and margin (Figs. 4B and 4C). Protodermal and underlying mesophyll precursors at the leaf margin appear enlarged and vacuolated and lack GUS activity (Figs. 4B and 4C). In cleared leaf preparations, GUS activity is observed in both pavement cell precursors and meristemoids of the protoderm layer (Fig. 4G), in palisade mesophyll precursors (Figs. 4E and 4H), and in procambium of all vein size classes (Figs. 4F and 4I).

At Day 8, a strong longitudinal gradient in GUS activity is apparent within the leaf blade (Figs. 5A and 5H–5L). In cross sections of the leaf blade base, GUS-expressing cells occur in

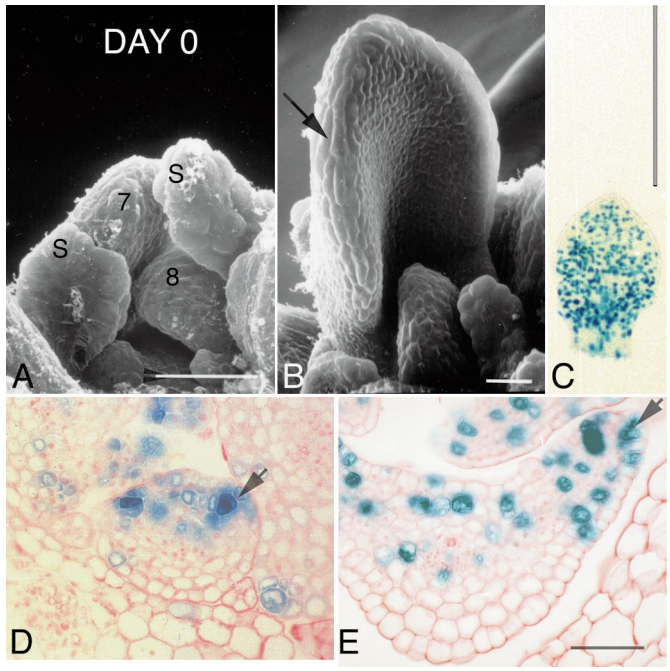

FIG. 3. Day 0 stage of *Arabidopsis* Leaf 8 development. (A and B) Scanning electron micrographs of *gl1* leaves. (A) Leaf 8 primordium (8) 50 μm in length. Also shown are Leaf 7 (7) and stipules (S) of older leaves. (B) Leaf 8 0.4 mm in length. Arrow indicates enlarged cells at margin. (C) Cleared leaf 250 μm in length. (D) Cross section of Historesin-embedded leaf primordium 50 μm in length. Arrow indicates GUS-expressing cell at margin. (E) Cross section of leaf 160 μm in length taken 25% (ca. 40μm) above the base. Arrow indicates GUS expression in marginal cell. Scale, 0.25 mm in C; 50 μm in A, B, D, and E.

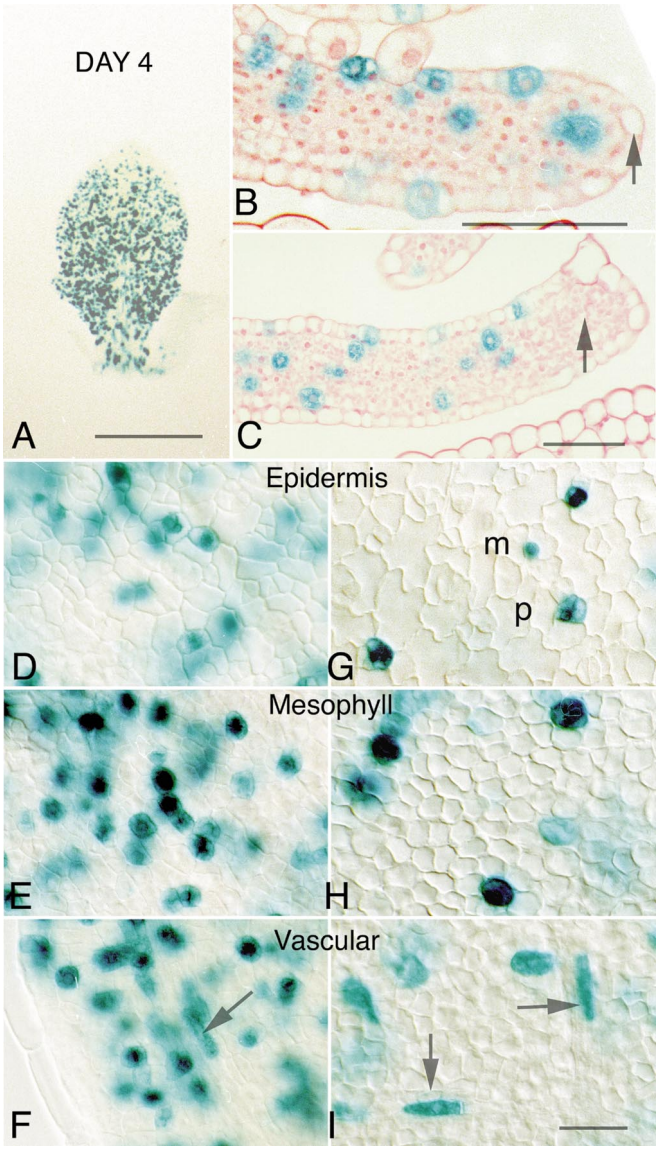

FIG. 4. Day 4 stage of *Arabidopsis* Leaf 8 development. (A) Cleared leaf 1.2 mm in length. (B and C) Cross sections of leaf 1.5 mm in length. (B) Section of Historesin-embedded tissue taken 25% (ca. 350 μm) above leaf base. (C) Section taken 50% (ca. 750 μm) above base. Arrows indicate absence of cycling cells at margin. (D–I) Photographs of cleared Day 4 leaves taken at 25% above base (D–F) and at 50% above base (G–I). Each photographic series (D–F, G–I) illustrates the same location at different focal planes. (D and G) Adaxial protoderm layer with meristemoid (m) and pavement (p) cells. (E and H) Palisade mesophyll precursor layer. (F and I) Procambial strands (arrows). Scale, 0.5 mm in A, 50 μm in B–I.

all tissue layers and are distributed in a diffuse pattern between margin and midrib (Figs. 5H and 5I). Cycling cells associated with procambial strand formation occur in the middle layer of mesophyll precursors (Fig. 5I). In the distal half of the blade, cycling cells are less frequent in the abaxial than in the adaxial layers of mesophyll precursor tissue (Figs. 5J–5L). Earlier cessation of cycling in abaxial mesophyll precursor layers is associated with cell enlargement, growth of plastids, and development of intercellular space within spongy mesophyll tissue (Figs. 5K and 5L). In cleared preparations, GUS labeling occurs in both epidermal pavement and meristemoid cells in the basal half of the blade, but becomes restricted to the meristemoids in the distal half (Figs. 5B and 5E). Density of GUS-accumulating palisade mesophyll precursor cells is high near the base of the blade, but reduced in the distal portion (Figs. 5C and 5F). GUS-labeled cells occur in the procambium of all vein size classes throughout the leaf blade (Figs. 5D and 5G; other data not shown).

At Day 12, the longitudinal gradient in GUS activity persists, with GUS labeling conspicuous only in the basal third of the lamina (Fig. 6A). The petiole elongates more rapidly at this stage (Fig. 2B) and displays strong GUS labeling. Protoderm and palisade mesophyll precursors from midlamina typically lack GUS-expressing cells (Fig. 6B). Cyclin accumulation in the protoderm is restricted to meristemoids (Fig. 6C). GUS labeling of palisade mesophyll cells is much less frequent, even near the blade base (Fig. 6D), although vein procambium still is labeled throughout the blade (Fig. 6E).

GUS labeling is sharply reduced in Day 16 and older leaf blades (Figs. 6F–6J, 7A, and 7B), but is still conspicuous in the petiole (Fig. 6F). GUS-expressing meristemoids are present in the adaxial protoderm layer of Day 16 leaf blades, but GUS activity was not observed in the palisade mesophyll at this and later stages (Figs. 6H and 6I). In Day 16 and a few Day 20 leaves, secondary vein procambial cells express GUS (Fig. 6J), and labeled cells are prominent in the basal half of the midvein (Figs. 6F, 7A, and 7C). GUS labeling was not observed in nonvascular tissues of the blade after Day 20, although labeled cells occurred in all tissues of the petiole until Day 28 (data not shown).

Differential Patterns of Cyclin Accumulation in Epidermis and Mesophyll

In Day 4 leaves, epidermal cyclin index values form a longitudinal gradient with slightly higher values near the blade base (Fig. 8A). The lower values near the apex coincide with a region where protoderm pavement cells have ceased to divide and only meristemoids express GUS (Fig. 8F). At Day 8, GUS is expressed in pavement cells only near the leaf base, while a majority of cycling cells in these positions and all those in the distal blade half are meristemoids (Figs. 8B and 8G). By Day 12, a strong longitudinal gradient in dermal cyclin index is apparent, with values of 0% at the tip of the leaf and the highest values observed, 6%, near the leaf base (Fig. 8C). Cessation of cell cycling in meristemoids occurs in an apex-to-base direction, with GUS-accumulating cells restricted to the basal 25% of the

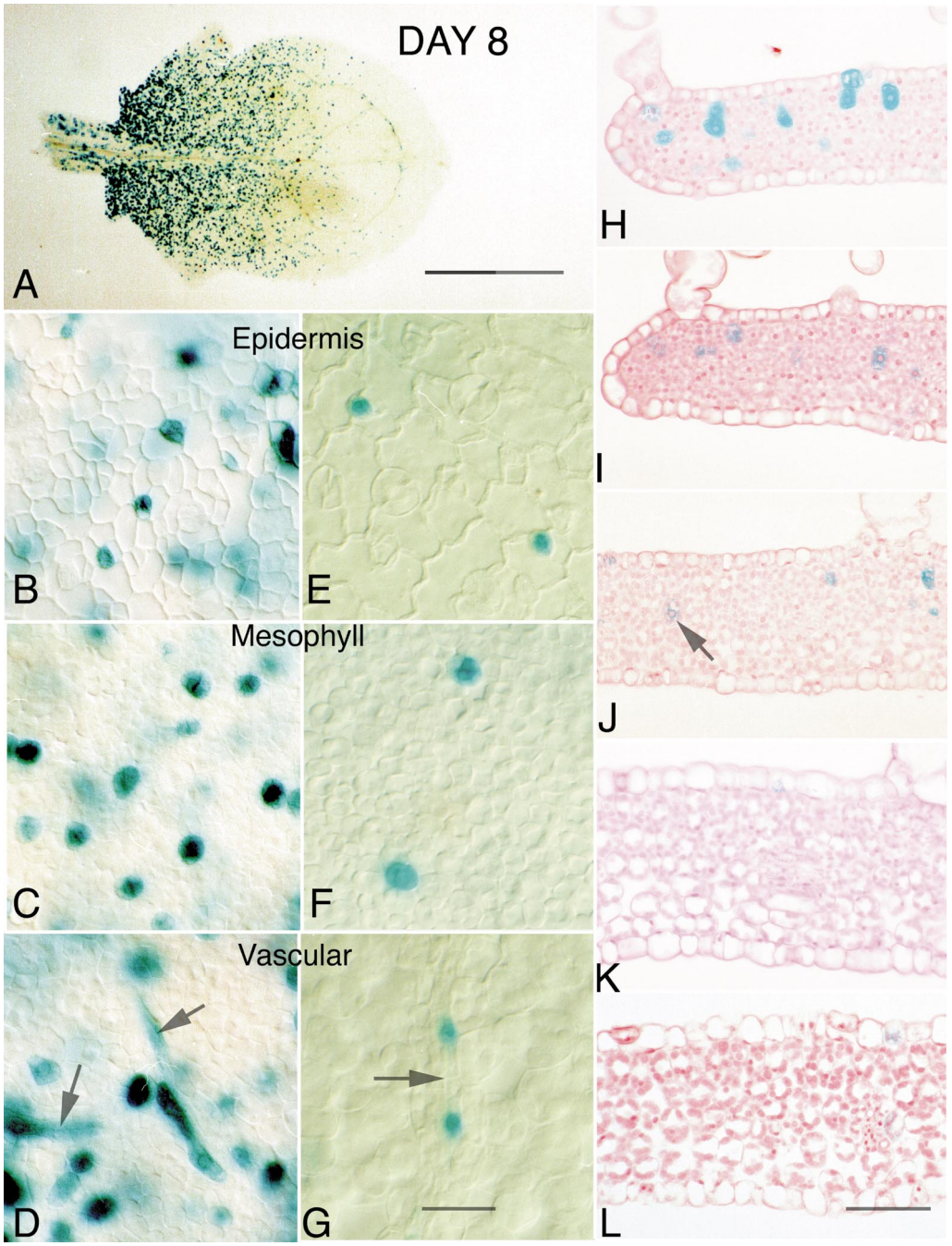

FIG. 5. Day 8 stage of *Arabidopsis* Leaf 8 development. (A) Cleared leaf 3.2 mm in length. (B–G) Photographs of cleared Day 8 leaves taken at position 25% above blade base (B–D) and 50% above blade base (E–G). Each photographic series (B–D, E–G) illustrates the same location at different focal planes. (B and E) Adaxial protoderm. (C and F) Palisade mesophyll layer. (D and G) Procambial strands (arrows). (H–L) Cross sections of Historesin-embedded tissue of Day 8 leaf 5 mm in length. (H) 0%, at blade base. (I) 25%, ca. 1 mm from blade base. (J) 50%, ca. 2 mm from blade base. Arrow indicates cycling associated with delimitation of procambium from middle mesophyll precursor layer. (K) 75%, ca. 3 mm from blade base. (L) 100%, near leaf apex. Scale, 1 mm in A, 50 μm in B–L.

leaf blade at Day 16 (Fig. 8D) and to the blade base (0%) at Day 20 (Fig. 8E); protoderm cell divisions were not observed after this stage.

Cyclin index values for the palisade mesophyll precursor layer show a longitudinal gradient from Day 4 to 12; no GUS-accumulating cells were observed in mesophyll tissue

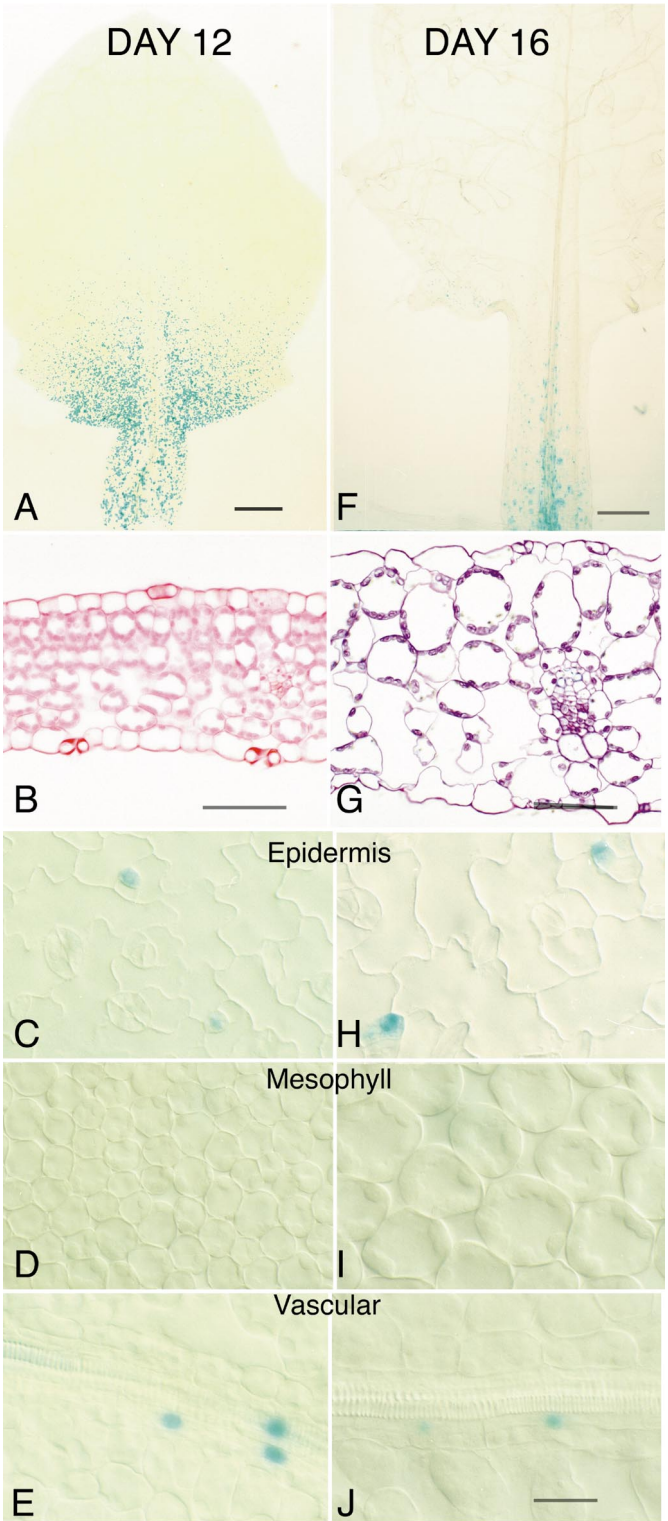

FIG. 6. Day 12 (A–E) and Day 16 (F–J) stages of *Arabidopsis* Leaf 8 development. (A) Cleared Day 12 leaf 8.2 mm in length. (B) Day 12 leaf cross section (Historesin-embedded tissue) at 50%, ca. 4 mm from blade base. (C–E, H–J). Photographs taken at position 25% above blade base and illustrating the same location on each leaf, but with different focal planes. (C and H) Adaxial protoderm. (D and I) Palisade mesophyll precursor layer. (E and J) Procambial strands. (F) Base of cleared Day 16 leaf 18 mm in length. (G) Day 16 leaf cross section (Spurr-embedded tissue) at 50%, ca. 9 mm from blade base. Scale, 1 mm in A, F; 50 μm in B–E, H–J.

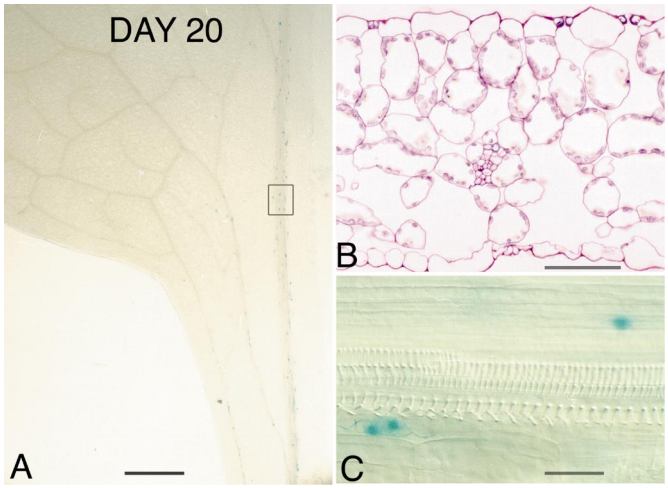

FIG. 7. Day 20 stage of *Arabidopsis* Leaf 8 development. (A) Cleared base of blade from leaf 26 mm in length. (B) Cross section (Spurr-embedded tissue) at 50% above blade base. (C) Midvein procambium from position indicated in A. Scale, 1 mm in A, 50 μm in B, C.

after this stage (Figs. 8A–8E). At Day 4, palisade mesophyll layer values are similar to the adaxial protoderm in the basal 50% of the blade, but are lower in the distal portion (Figs. 8A and 8B); a similar relationship holds in Day 8 leaves (Fig. 8B). Nevertheless, palisade layer cycling continues beyond that of dermal pavement cells: dermal layer divisions become restricted to stomate-forming meristemoids after Day 8, while palisade layer cycling continues through Day 12 (Fig. 8C).

Temporal and Spatial Patterns of Cell Enlargement

Distribution patterns of cell enlargement are complementary to those of cell division: as the proportion of cells that are cycling decreases, observable cell enlargement increases. Prior to Day 4, protodermal cells are polygonal in shape and uniform in area (Figs. 3B and 3D) but by Day 4, protodermal cells become heterogeneous in size, with formation of the first guard cell pairs and of sinuous pavement cells (Figs. 4G and 9A). At Day 8 there is a strong longitudinal gradient in dermal cell size, with small polygonal cells at the leaf base and enlarged sinuous pavement cells and

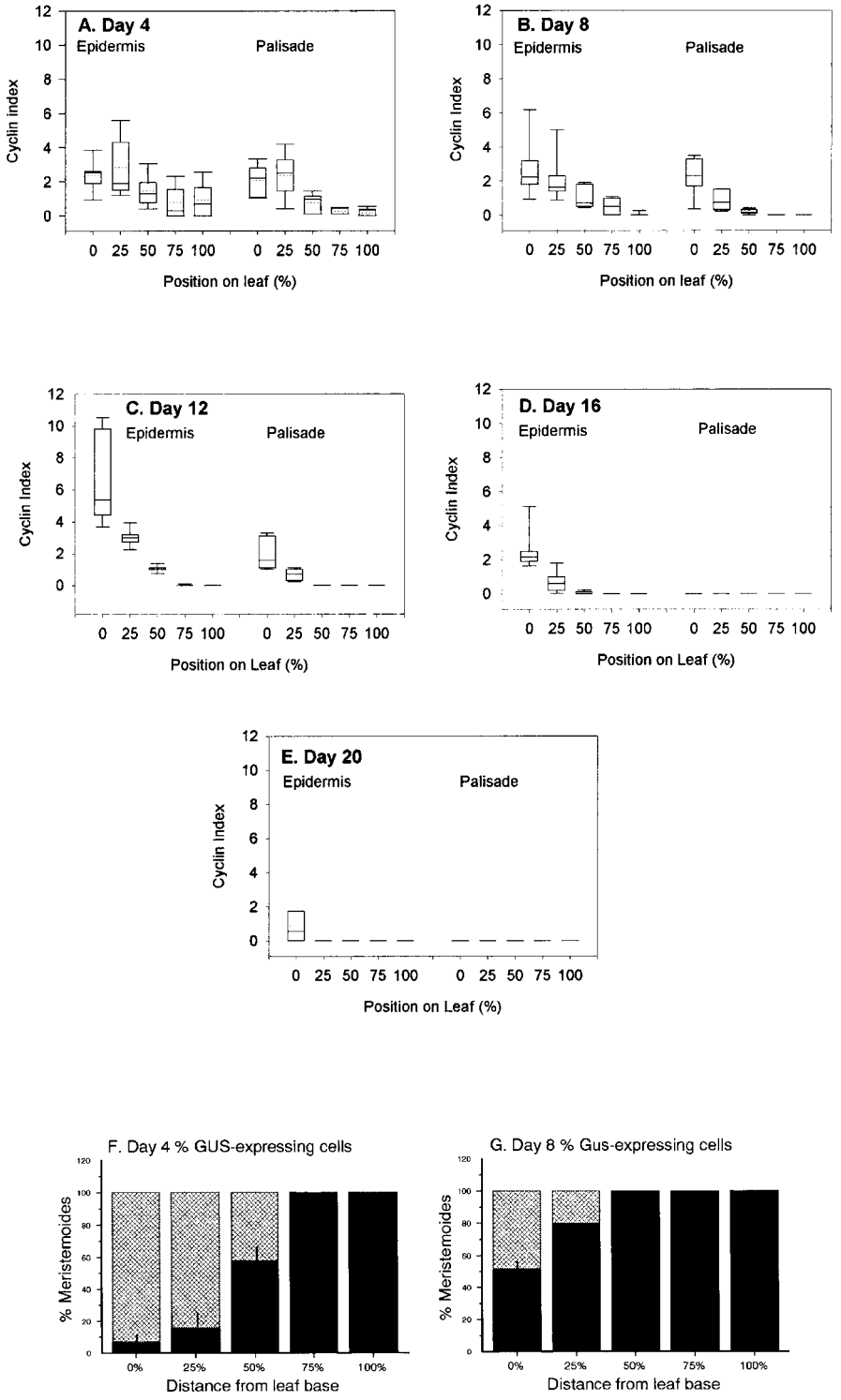

FIG. 8. Cyclin indices for adaxial epidermal and palisade mesophyll layers at five positions (0, 25, 50, 75, and 100% of the distance from blade base to apex) in developing *Arabidopsis* leaves. Graphs A–E represent variation in cyclin index data for each sampling date. Solid line within box represents 50th percentile; box delimits 25th and 75th percentiles; bars indicate 10th and 90th percentiles. Dotted line indicates mean. (A) Day 4. (B) Day 8. (C) Day 12. (D) Day 16. (E) Day 20. Graphs F and G represent proportion of GUS-expressing cells in adaxial dermal layer that are meristemoids (black) or pavement cells (cross-hatched). (F) Day 4. (G) Day 8.

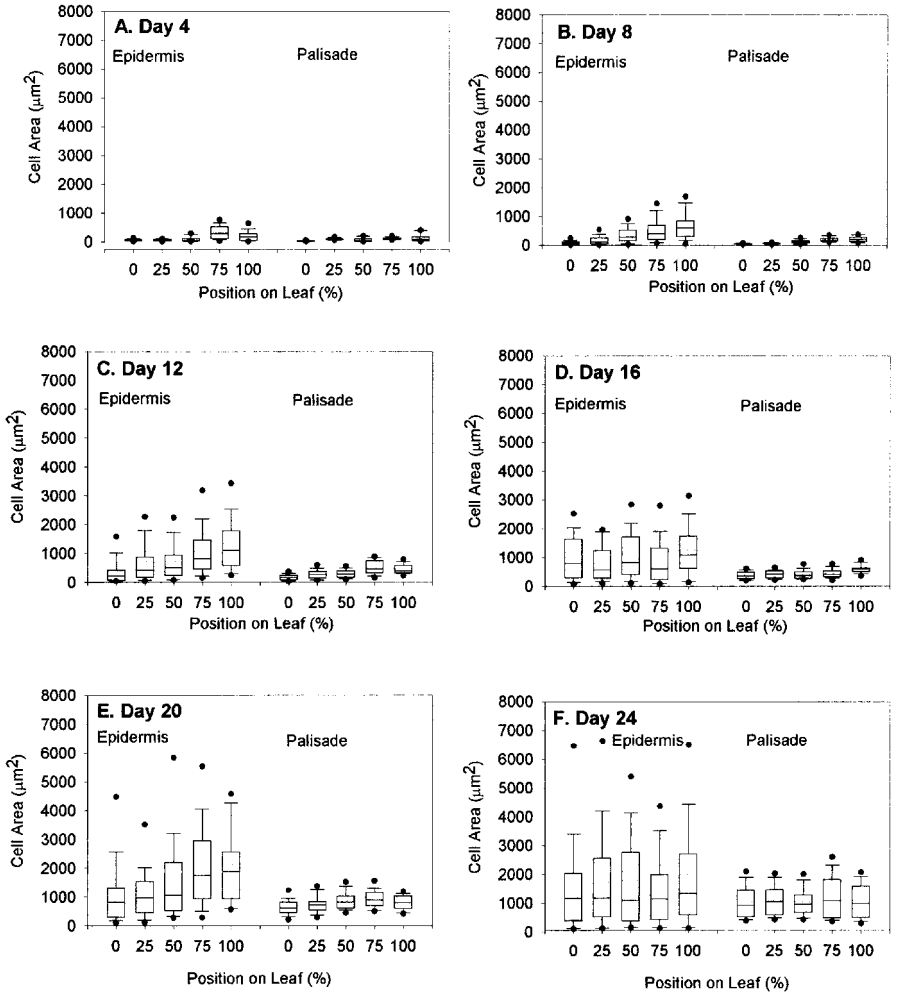

FIG. 9. Cell area of adaxial epidermal and palisade mesophyll cells in developing leaves of *Arabidopsis.* Graphs represent variation in cell area data for each sampling date. Plots as in Fig. 8. Dots indicate data lying outside the 10th and 90th percentiles. (A) Day 4. (B) Day 8. (C) Day 12. (D) Day 16. (E) Day 20. (F) Day 24.

stomata in the distal 75% of the blade length (Figs. 5B, 5E, and 9B). By Day 12, protoderm cell size still displays a longitudinal gradient, but stomata and enlarged pavement cells are now present in the basal 25% of blade length (Figs. 6C and 9C). The longitudinal gradient becomes dampened by Day 16 and after, as cells near the base of the leaf "catch up" to cells in the distal portion (Figs. 6H and 9D–9F). Size heterogeneity of dermal tissue is indicated by the extent of the 90th percentile and by the range of outlier points, of which the largest outlier points represent giant pavement cells and the smallest meristemoids or their recent derivatives (Figs. 9C–9F).

The pattern of palisade cell enlargement differs strikingly: longitudinal gradients are present up to Day 16, but cell shape is more uniform, with little variance within each location sampled on the leaf blade (Figs. 4E, 4H, 5C, 5F. 6D, 6I, and 9A–9F). Precursors of the palisade mesophyll are polygonal in shape in the basal half of Day 4 and younger leaves (Figs. 3E, 4B, 4C, and 4E). As palisade mesophyll cells begin to enlarge, they become circular in surface view and intercellular space begins to form (Figs. 4H, 5F, 6D, and 6I). Stomatal formation in the adjacent dermal layer coincides with the beginning of intercellular space formation in the palisade mesophyll layer (Figs. 4G and 4H). Palisade cells undergo most enlargement after Day 16, including elongation in the dorsoventral plane (Figs. 9E and 9F).

DISCUSSION

Role of Marginal Meristem in Leaf Organogenesis

The defining feature of typical dicot leaves is formation of the dorsoventrally flattened leaf blade in the distal portion of the primordium. Although blade inception has long been

attributed to the division activity of the "marginal meristem," the spatial extent and temporal duration of its activity have been controversial (Maksymowych and Wochok, 1969; Cusset, 1986; Poethig and Sussex, 1986). In this study we observed strong and localized GUS activity in cells in a marginal position in Day 0 primordial leaves (Figs. 10A and 10B). Cycling was never restricted to the margin, however, and cells in this position ceased cycling long before those of other leaf tissues. Although the absence of *cyc1At::GUS* expression at the leaf margin has been illustrated on a more macroscopic scale for the older first leaves of *Arabidopsis* (Van Lijsebettens and Clarke, 1998), our study is the first to directly observe spatial and temporal patterns of cycling in the marginal meristem on a microscopic scale. We show that the altered growth direction during blade inception is temporally coincident with cell cycling within the marginal meristem and hypothesize that cell division is prerequisite for the initial formation of the leaf blade. The mutant phenotypes of the *argonaute1* mutation of *Arabidopsis* (Bohmert *et al.*, 1998) and the *lamina-1* mutation of *Nicotiana* (McHale, 1993) indicate that these wild-type genes have a role in blade formation, possibly in this ephemeral, but crucial, morphogenetic activity of the marginal meristem. A second hypothesized role for the marginal meristem has been generation of tissue layers (Avery, 1933; Foster, 1936; Esau, 1965). We saw no evidence for this histogenetic role of the marginal meristem and conclude that the regular array of tissue layers is generated solely through regulation of the diffuse pattern of anticlinal divisions that defines plate meristem activity (Fig. 10C).

Basiplastic Gradient of Cell Cycling

Patterns of cell cycling related to morphogenesis of the leaf blade, tissue proliferation, and differentiation of specific cell types all occur along a striking longitudinal gradient (Fig. 10D). Two major patterns are known to occur in leaves of higher plants: (1) acroplastic, in which cell maturation proceeds from base to apex, and (2) basiplastic, in which processes proceed from apex to base. Only a few acroplastic patterns are well documented among the flowering plants, while basiplastic patterns are more common. In our study of temporal and spatial patterns of cell cycling in expanding leaves of *Arabidopsis*, the overall expression of the *cyc1At::GUS* construct was strikingly basiplastic (Figs. 10E–10G). Cycling cells initially are observed throughout the leaf, but gradually become restricted to more basal portions of the blade and then to the petiole, as inferred from earlier studies of *Arabidopsis* and other dicots (e.g., Avery, 1933; Maksymowych, 1963; Tsuge *et al.*, 1996). The appearance of mitotic figures in sectioned tissue (Pyke *et al.*, 1991) and the macroscopic expression pattern of a *cyclin::GUS* reporter gene (Van Lijsebettens and Clarke, 1998) in the first rosette leaf of *Arabidopsis* provided direct evidence for the longitudinal gradient, but our study is the first to provide a detailed analysis and to relate whole leaf patterns with specific tissue types.

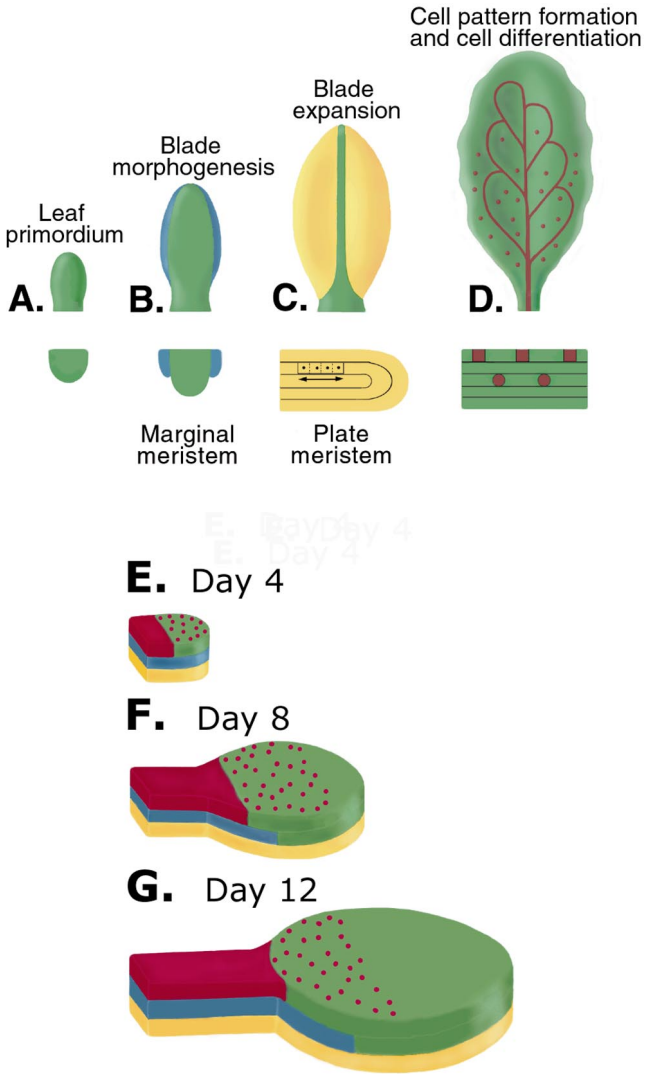

FIG. 10. Diagrams illustrating stages of leaf development in *Arabidopsis*. (A) Leaf primordium. (B) Blade morphogenesis associated with marginal meristem activity (blue). (C) Blade expansion associated with plate meristem activity (yellow). (D) Cell pattern formation and cell differentiation within tissue layers, including stomatal and vein precursors (red).Top row, surface view; bottom row, cross-sectional view. Diagrams summarizing tissue layer-specific patterns of cell cycling in developing leaves of *Arabidopsis*. (E) Day 4. (F) Day 8. (G) Day 12. Cycling related to stomatal guard cell formation (red dots) and differentiation of vascular tissue (yellow circles and lines) is superimposed on the more general spatial patterns of cell proliferation within the adaxial epidermal (red) and palisade mesophyll (blue) layers.

Tissue Layer Proliferation

Individual tissue layers are maintained during leaf expansion by the predominance of anticlinal divisions during plate meristem activity. Our observations show that both

adaxial protoderm and palisade mesophyll precursor layers display a basiplastic gradient in division pattern, but that frequency of cell cycling differs between them from the early stages of lamina expansion (Figs. 10E–10G). Proliferative cell division occurs in a greater portion of the leaf blade and over a longer period of time in the palisade precursor layer compared with the epidermal layer. This overall pattern has been inferred for other species either from indirect observations of cell size and cell number (Avery, 1933; Maksymowych, 1963) or from direct observations of the distribution of mitotic figures (Dale, 1964; Denne, 1966). The differences between dermal and mesophyll layers indicate that, while the basic mechanism of cell cycling is presumably common to both tissue layers, regulatory pathways must differ. In *Arabidopsis,* support for tissue layer-specific regulatory pathways comes from the *pale cress* mutant in which palisade mesophyll cell number per unit volume is reduced by 50%, but adjacent epidermis is unaffected (Reiter *et al.,* 1994).

Cell Differentiation

Within the dermal layer, differential spatial and temporal patterns of expression of the *cyc1At::GUS* construct differ for meristemoids and pavement cells. Primary meristemoids are formed when a dermal precursor cell divides asymmetrically; the smaller derivative, the meristemoid, typically divides several times before giving rise to a guard cell mother cell (Larkin *et al.,* 1997; Serna and Fenoll, 1997). Secondary or satellite meristemoids are formed in *Arabidopsis* and several other dicotyledons when a pavement cell adjacent to a stomate divides asymmetrically. In our study, stomates were always observed in regions where dermal pavement had ceased division, indicating that most GUS-accumulating meristemoids were secondary. Expression of a *cyc1aAt::GUS* construct in meristemoids of *Arabidopsis* leaves was previously shown by Serna and Fenoll (1997), but they were interested specifically in development of stomata and stomatal clusters rather than spatial and temporal patterns of cell cycling on a whole leaf basis.

Other specialized cell types in the epidermis of *Arabidopsis* leaves include trichomes and the associated ring of trichome support cells. In *Arabidopsis,* trichomes do not arise from asymmetric divisions and, once initiated, do not divide (Larkin *et al.,* 1997). In our material, trichome precursors were detectable morphologically in developing leaves, but did not express the *cyc1At::GUS* construct. *Arabidopsis* leaf trichome cells have elevated ploidy levels, ranging from 4C to 64C (Melaragno *et al.,* 1993), indicating that these cells repeatedly cycle through S phase. The fact that these endopolyploid cells did not express GUS is further evidence that B-type cyclins, such as *cyc1At,* accumulate specifically during the G2 and M, but not the G1 and S phases of the cycle. In contrast, trichome support cells were observed to express GUS (not illustrated); these cells are formed from normal pavement cells adjacent to trichome cells by a series of radially oriented cell divisions. Thus, trichome support cells appear to be completing the full cell cycle, passing through G2 and M phases and undergoing cytokinesis, while trichome cells bypass these phases and undergo spectacular overall increase in volume.

Within *Arabidopsis* leaf blades, cell cycling continues longest in the precursor of the vascular tissue, the procambium. During leaf expansion, leaf veins are formed in an hierarchical order, with midvein formed first, followed by secondary veins with their connecting loops, and then the smaller tertiary and quaternary veins that make up reticulate fine venation (Telfer and Poethig, 1994; Nelson and Dengler, 1997; Kinsman and Pyke, 1998; Candela *et al.,* 1999). While midvein procambium is formed from base to apex, subsequently formed veins appear in an apex-to-base direction, conforming to the overall basiplastic pattern of tissue development and leaf expansion. Vein pattern is formed very early in leaf development (Nelson and Dengler, 1997; Candela *et al.,* 1999), but differentiation of vascular tissues from their procambial precursors may continue for an extended period of time. In addition, bundle sheath cells are delimited from the ground tissue at the periphery of leaf veins in *Arabidopsis,* a process that probably requires precisely oriented division planes (Kinsman and Pyke, 1998). Our observations of GUS-expressing cells in vein procambium at late stages of *Arabidopsis* leaf development likely reflect these and other divisions required for vascular differentiation and indicate that this construct has potential for elucidating relationships between cell division and vascular differentiation.

Cell Cycling and Cell Size

Cell size is determined by the interaction of whole organ expansion and cell division. Genetic manipulation of this interaction, such as by dominant negative mutations of the *cdc2* gene that repress cell division, show that plant morphogenesis and histogenesis proceed more or less normally despite disruption of the normal balance between cell size and cell division (Hemerly *et al.,* 1995). Although plant development is highly flexible and can accommodate substantial perturbation, the predictable patterns of cell size, even within dividing tissues such as the shoot apical meristem, indicate that cell sizer controls may operate in plants as well as in microorganisms (John *et al.,* 1993a,b; Francis and Halford, 1995; Francis 1998). Francis (1998) proposed a model for cell size control of cycling in which: (1) a minimum size is required for commitment to cell division, (2) a critical size provides a checkpoint for the cell cycle (or is at least a marker of an optimal level of regulatory proteins), and (3) there are tissue-specific sizer controls. Our study provides circumstantial support for the first and third of these tenets. In expanding leaves of *Arabidopsis,* populations of dermal and mesophyll cells with relatively high cycling rates maintained a constant cell size (ca. 75 μm^2), regardless of position on the leaf, developmental stage, or tissue type. Moreover, there were striking differences between the two tissue layers examined in the size at

which cells exit the cycle. Palisade mesophyll cells cease cycling when they are about 200 μm^2 in area (see also Kim *et al.*, 1998) and continue to expand 4- to 5-fold. In contrast, dermal pavement cells exit the full mitotic cycle when mean size is about twice as large, 400 μm^2, and at least some cells continue to expand up to 16-fold. The direct relationship between ploidy level and pavement cell area (Melaragno *et al.*, 1993) indicates that cell size controls may operate on entry into S phase, but may be uncoupled in a stochastic way from G2 and M phase so that only a portion of cells complete the full cycle. The distribution of cell sizes in dermal tissue is further complicated by the superposition of cycling related to stomatal formation upon more general proliferative cell divisions. Thus, not only do size controls on cell cycling differ between tissue layers, but they also differ among cell types within layers.

Our detailed analysis of cell cycling during leaf development in the model genetic organism *Arabidopsis* provides a baseline for mutant characterization (e.g., Kim *et al.*, 1998) and prerequisite information for identifying the multiple signaling pathways required to coordinate cell division behavior within a developing plant organ. Further, as leaves represent a developmental ground state for sepals, petals, stamens, and carpels, the patterns described here have general applicability to morphogenesis and expansion of all determinate organs in plants. Similarities between cell cycle mutant phenotypes in *Arabidopsis*, *Drosophila* (e.g., Weigmann *et al.*, 1998), and other model organisms also indicate that common principles may govern the relationships between cell cycling, organogenesis, and cell differentiation across major clades of multicellular organisms.

ACKNOWLEDGMENTS

We thank John L. Celenza for the gift of the *cyc1At::GUS* reporter construct and Thomas Berleth for helpful discussion.

REFERENCES

Avery, G. S. (1933). Structure and development of the tobacco leaf. *Am. J. Bot.* **20,** 565–592.

Bohmert, K., Camus, I., Bellini, C., Bouchez, D., Caboche, M., and Benning, C. (1998). *AGO1* defines a novel locus of *Arabidopsis* controlling leaf development. *EMBO J.* **17,** 170–180.

Candela, H., Martinez-Laborda, A., and Micol, J.-L. (1999). Venation pattern formation in *Arabidopsis thaliana* vegetative leaves. *Dev. Biol.* **205,** 205–216.

Cleveland, W. S. (1985). "The Elements of Graphing Data." Wadsworth, Monterey, CA.

Cusset, G. (1986). La morphogenèse du limbe des Dicotyledonés. *Can. J. Bot.* **64,** 2807–2839.

De Block, M., and Van Lijsebettens, M. (1997). β-Glucuronidase enzyme histochemistry on semithin sections of plastic-embedded *Arabidopsis* explants. *In* "Methods in Molecular Biology: *Arabidopsis* Protocols" (J. Martinez-Zapater and J. Salinas, Eds.), Vol. 82, pp. 397–407. Humana Press, Clifton, NJ.

Denne, M. P. (1966). Leaf development in *Trifolium repens*. *Bot. Gaz.* **127,** 202–210.

DeVeylder, L., Van Montagu, M., and Inzé, D. (1998). Cell cycle control in *Arabidopsis*. *In* "Plant Cell Division" (D. Francis, D. Dudits, and D. Inzé, Eds.), pp. 1–19. Portland Press, London.

Doerner, P., Jorgensen, J., You, R., Steppuhn, J., and Lamb, C. (1996). Control of root growth and development by cyclin expression. *Nature* **380,** 520–523.

Drews, G. N., and Okamura, J. K. (1996). *In situ* hybridization with nonradioactive probes. *In* "Cold Spring Harbor *Arabidopsis* Molecular Genetics Course Manual." Cold Spring Harbor Laboratory Press, Cold Spring Harbor, NY.

Esau, K. (1965). "Plant Anatomy". Wiley, New York.

Ferreira, P., Hemerly, A., de Almeida Engler, J., Bergounioux, C., Burssens, S., Van Montagu, M., Engler, G., and Inzé, D. (1994a). Three discrete classes of *Arabidopsis* cyclins are expressed during different intervals of the cell cycle. *Proc. Natl. Acad. Sci. USA* **91,** 11313–11317.

Ferreira, P. C. G., Hemerly, A. S., de Almeida Engler, J., Van Montagu, M., Engler, G., and Inzé, D. (1994b). Developmental expression of the *Arabidopsis* cyclin gene *cyc1At*. *Plant Cell* **6,** 1763–1774.

Fobert, P. R., Coen, E. S., Murphy, G. J. P., and Doonan, J. H. (1994). Patterns of cell division revealed by transcriptional regulation of genes during the cell cycle in plants. *EMBO J.* **13,** 616–624.

Foster, A. S. (1936). Leaf differentiation in angiosperms. *Bot. Rev.* **2,** 349–372.

Francis, D. (1998). Cell size and organ development in higher plants. *In* "Plant Cell Division" (D. Francis, D. Dudits, and D. Inzé, Eds.), pp. 187–206. Portland Press, London.

Francis, D., and Halford, N. G. (1995). The plant cell cycle. *Physiol. Plant* **93,** 365–374.

Hemerly, A., Bergounioux, C., Van Montagu, M., Inze, D., and Ferreira, P. (1992). Genes regulating the plant cell cycle: Isolation of a mitotic-like cyclin from *Arabidopsis thaliana*. *Proc. Natl. Acad. Sci. USA* **89,** 3295–3299.

Hemerly, A., de Almeida Engler, J., Bergounioux, C., Van Montagu, M., Engler, G., Inze, D., and Ferreira, P. (1995). Dominant negative mutants of the Cdc2 kinase gene uncouple cell division from iterative plant development. *EMBO J.* **14,** 3925–3936.

Kim, G.-T., Tsukaya, H., and Uchimiya, H. (1998). The CURLY LEAF gene controls both division and elongation of cells during the expansion of the leaf blade in *Arabidopsis thaliana*. *Planta* **206,** 175–183.

Kinsman, E. A., and Pyke, K. (1998). Bundle sheath cells and cell-specific plastid development in *Arabidopsis* leaves. *Development* **125,** 1815–1822.

Kouchi, H., Sekine, M., and Hata, S. (1995). Distinct classes of mitotic cyclins are differently expressed in the soybean shoot apex during the cell cycle. *Plant Cell* **7,** 1143–1155.

Larkin, J. C., Marks, M. D., Nadeau, J., and Sack, F. (1997). Epidermal cell fate and patterning in leaves. *Plant Cell* **9,** 1109–1120.

Maksymowych, R. (1963). Cell division and cell elongation in leaf development of *Xanthium pennsylvanicum*. *Am. J. Bot.* **50,** 891–901.

Maksymowych, R., and Wochok, Z. S. (1969). Activity of marginal and plate meristems during leaf development of *Xanthium pennsylvanicum*. *Am. J. Bot.* **56,** 26–30.

McHale, N. A. (1993). *LAM-1* and *FAT* genes control development of the leaf blade in *Nicotiana sylvestris*. *Plant Cell* **5,** 1029–1038.

Melaragno, J. E., Mehrotra, B., and Coleman, A. W. (1993). Relationship between endopolyploidy and cell size in epidermal tissue of *Arabidopsis*. *Plant Cell* **5,** 1661–1668.

Nelson, T., and Dengler, N. G. (1997). Leaf vascular pattern formation. *Plant Cell* **9,** 1121–1135.

Poethig, R. S., and Sussex, I. M. (1985). The cellular parameters of leaf development in tobacco: A clonal analysis. *Planta* **165,** 170–184.

Pyke, K. A., Marrison, J. L., and Leech, R. M. (1991). Temporal and spatial development of the cells of the expanding first leaf of *Arabidopsis thaliana* (L.) Heynh. *J. Exp. Bot.* **42,** 1407–1416.

Reiter, R. S., Coomber, S. A., Bourett, T. M., Bartley, G. E., and Scolnik, P. A. (1994). Control of leaf and chloroplast development by the *Arabidopsis* gene *pale cress*. *Plant Cell* **6,** 1253–1264.

Renaudin, J., Doonan, J. H., Freeman, D., Hashimoto, J., Hirt, H., Inzé, D., Jacobs, T., Kouchi, H., Rouze, P., Sauter, M., Savoure, A., Sorrell, D. A., Sundaresan, V., and Murray, J. A. H. (1996). Plant cyclins: A unified nomenclature for plant A-, B- and D-type cyclins based on sequence organization. *Plant Mol. Biol.* **32,** 1003–1018.

Serna, L., and Fenoll, C. (1997). Tracing the ontogeny of stomatal clusters in *Arabidopsis* with molecular markers. *Plant J.* **12,** 747–755.

Shaul, O., Van Montagu, M., and Inzé, D. (1996a). Cell cycle control in *Arabidopsis*. *Ann. Bot.* **78,** 283–288.

Shaul, O., Mironov, V., Burssens, S., Van Montagu, M., and Inzé, D. (1996b). Two *Arabidopsis* cyclin promoters mediate distinctive transcriptional oscillation in synchronized tobacco BY-2 cells. *Proc. Natl. Acad. Sci. USA* **93,** 4868–4872.

Smith, L. G. (1996). What is the role of cell division in leaf development? *Semin. Cell Dev. Biol.* **7,** 839–848.

Telfer, A., and Poethig, R. S. (1994). Leaf development in *Arabidopsis*. *In* "*Arabidopsis*" (E. M. Meyerowitz and C. R. Somerville, Eds.), pp. 379–401. Cold Spring Harbor Laboratory Press, Plainview, NY.

Tsuge, T., Tsukaya, H., and Uchimiya, H. (1996) Two independent and polarized processes of cell elongation regulate leaf blade expansion in *Arabidopsis thaliana* (L.) Heynh. *Development* **122,** 1589–1600.

Van Lijsebettens, M., and Clarke, J. (1998). Leaf development in *Arabidopsis*. *Plant Physiol. Biochem.* **36,** 47–60.

Weigmann, K., Cohen, S. M., and Lehner, C. F. (1997). Cell cycle progression, growth and patterning in imaginal discs despite inhibition of cell division after inactivation of *Drosophila* Cdc2 kinase. *Development* **124,** 3555–3563.

Received for publication June 10, 1999
Revised August 9, 1999
Accepted August 9, 1999